

Modelling soil-water interaction with the Material Point Method. Evaluation of single-point and double-point formulations

F. Ceccato

University of Padua, Italy

A. Yerro

Virginia Tech, Blacksburg, US

M. Martinelli

Deltares, Delft, The Netherlands

ABSTRACT: Many problems in geotechnical engineering involve large deformations and soil-water interactions, which pose challenging issues in computational geomechanics. In the last decade, the Material Point Method (MPM) has been successfully applied in a number of large-deformation geotechnical problems and multiphase MPM formulations have been recently proposed. In particular, there exist two advanced coupled hydro-mechanical MPM approaches to model the interaction between solid grains and pore fluids: the single-point and the double-point formulation. The first discretizes the soil-water mixture with a single set of material points (MP) which moves according to the solid velocity field. The latter uses two sets of MP one for the fluid phase and the other for the solid phase and they move according to the respective velocity field. The aims of this work is to present and compare the two theories, to emphasize their limitations and potentialities, and to discuss their applicability in the geotechnical field. To this end, the results of two numerical examples carried out by using both formulations are presented: a 1D-consolidation problem and a saturated column collapse problem.

1 INTRODUCTION

Soil-water interaction problems are of great interest in the field of geotechnical engineering. Underground excavations, pile installations, seepage failures, slope instabilities and landslides are just a few examples. In many cases, the material involved can experience large deformations, which might lead to dramatic events endangering human lives.

The numerical simulation of these problems is challenging because the treatment of large deformations, interactions between solid and fluid, and fluidization and sedimentation processes is not straightforward.

Large deformations can be effectively simulated with the Material Point Method (MPM) (Sulsky et al., 1994), which is a continuum-based technique that discretizes the media into a set of Lagrangian material points (MP), which move attached to the material and carry all the updated information such as velocities, strain, stresses, and history variables. Large deformations are simulated by MPs moving through a computational nodal grid that covers the full problem domain. The main governing equations are solved incrementally at the nodes of this grid that typically re-

mains fixed throughout the calculation. Variables required at the mesh to solve the governing equations are transferred from MPs to the nodes using mapping functions. The same mapping functions are used to update the quantities carried by the MPs by interpolation of the mesh results. This dual description of the media, i.e. MPs and nodal grid, prevents mesh distortion problems hence re-meshing techniques are not required. In addition, the original 1-phase MPM-formulation has the advantage that the mass is automatically conserved because the total mass of each MP remains constant through the calculation.

The need of taking into account the interaction between soil and pore fluids brought to the development of multi-phase MPM-formulations. Within the recent years, several approaches were presented in the literature to model coupled hydro-mechanical 2-phase (e.g., saturated soils) (Zabala & Alonso, 2011; Jassim et al. 2013, Abe et al., 2013, Bandara & Soga, 2015, Martinelli, 2016) and 3-phase (e.g., partially saturated soils) (Yerro et al., 2015) problems (Figure 1).

The interaction between two phases is formulated essentially in two different manners: adopting either one set of MPs (i.e., single-point approach, see Section 2) or two separate sets of MPs (i.e., double-point approach, see Section 3).

The aim of this paper is to compare the two formulations emphasizing their limitations and potentialities in different geotechnical applications. Two numerical examples are presented in order to validate and compare the results of both theories. The first example (Sec. 4.1) considers a 1D consolidation problem, while the second (Sec. 4.2) simulates the collapse of a water saturated column.

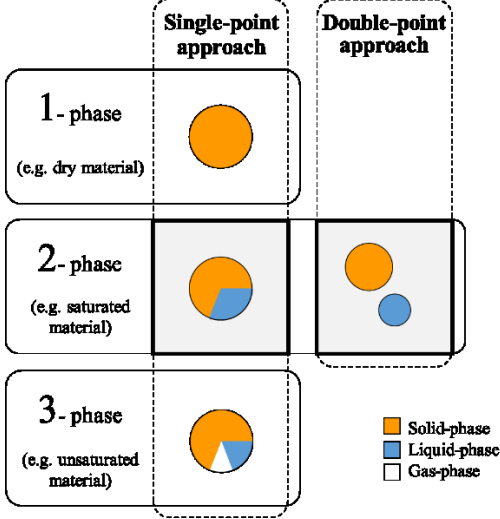


Figure 1 Scheme of multi-phase MPM-formulations (modified from Yerro et al. (2015)).

2 2-PHASE, SINGLE-POINT FORMULATION

The single-point formulation (Zabala & Alonso, 2011; Jassim et al. 2013) considers only one set of MPs. Each MP represents a portion of saturated porous media and carries the information of the solid (solid skeleton) and liquid in the pores (e.g. water). In this case, the MPs remain attached to the solid skeleton giving a Lagrangian description of the solid-phase movement, while the liquid-phase behaviour is described with respect the MPs by means of an Eulerian approach.

This formulation has been successfully applied to the simulation of CPT in partially drained conditions (Ceccato et al. 2016a,b; Galavi et al., 2017), and to model landslides and slope failures (Alonso et al, 2014, Soga et al. 2015; Yerro et al. 2016).

This work uses the approach proposed by Jassim et al. (2013), in which dynamic momentum balances of the liquid phase (Eq.1) and the mixture (Eq.2) are the governing equations posed at the nodes. In this case, all dynamic terms are taken into account, and \mathbf{a}_S and \mathbf{a}_L are the primary unknowns. Solid and total mass balances (Eq.3 and 4), as well as constitutive relationships are solved at the MPs.

$$\rho_L \mathbf{a}_L = \nabla p - \mathbf{f}^d + \rho_L \mathbf{b} \quad (1)$$

$$n_S \rho_S \mathbf{a}_S + n_L \rho_L \mathbf{a}_L = \nabla \cdot \boldsymbol{\sigma} + \rho_m \mathbf{b} \quad (2)$$

$$\frac{D^S n_L}{Dt} = n_S \nabla \cdot \mathbf{v}_S \quad (3)$$

$$\frac{D^S \varepsilon_{vol,L}}{Dt} = \frac{1}{n_L} [n_S \nabla \cdot \mathbf{v}_S + n_L \nabla \cdot \mathbf{v}_L] \quad (4)$$

where n_S =volumetric concentration ratio of solid, n_L =volumetric concentration ratio of liquid (equivalent to porosity in saturated soils), ρ_S = solid density, ρ_L =liquid density, ρ_m =density of the mixture, \mathbf{v}_S and \mathbf{v}_L are the solid and liquid velocities, $\boldsymbol{\sigma}$ =Cauchy total stress tensor, \mathbf{f}^d =drag force, and $\varepsilon_{vol,L}$ =volumetric strain of liquid-phase. $D^S(\cdot)/Dt$ denotes the material time derivative with respect to the solid phase.

In this approach, the flow is considered laminar and stationary in slow velocity regime, hence the interaction force between solid and liquid phases (i.e. drag force \mathbf{f}^d , term in Eq.1) is governed by Darcy's law (Eq.5). This hypothesis can be controversial in high velocity flows where drag forces may become nonlinear as better explained in the following.

$$\mathbf{f}^d = \frac{n_L \mu_L}{\kappa_L} (\mathbf{v}_L - \mathbf{v}_S) \quad (5)$$

In Equation 5 μ_L is the dynamic viscosity of the liquid and κ_L the liquid intrinsic permeability, which are assumed constant throughout the simulation.

Equation 3 is the expression for the mass balance of the solid and is used to update the porosity according to volumetric deformation of the solid skeleton.

In the framework of the 2-phase single-point approach, solid mass conservation is automatically fulfilled because the solid mass remains constant in each MP. However, this condition is not naturally satisfied for the liquid, because liquid can move apart from the solid skeleton depending on solid volumetric strain changes (porosity changes). Consequently, liquid mass in MPs can change and the conservation of the liquid mass is totally controlled by the accuracy in which the liquid mass balance is solved. Fluxes due to spatial variations of liquid mass are neglected in the 2-phase single-point formulation ($\nabla n_L \rho_L \approx 0$), hence the total mass balance results in Equation 4, and describes the volumetric strain rate of the liquid-phase. This hypothesis is reasonable when gradients of porosity are relatively small, but can induce errors when two materials with very different porosity are in contact. In addition, to obtain Equation 4, liquid is assumed to be weakly compressible.

Finally, constitutive relationships for solid and liquid are solved at the MPs to update stresses and pore pressure. The water is assumed linearly compressible via the bulk modulus of the fluid K_L and shear stresses in the liquid phase are neglected.

As usual in MPM, Equations 1 and 2 are discretized in space by means of the Galerking method and solved in time with a semi-explicit time discretization scheme.

The MPM solution scheme for each time step can be summarized as follow:

- 1) Liquid nodal acceleration \mathbf{a}_L is calculated by solving the discretized form of Equation 1.

- 2) \mathbf{a}_L is subsequently used to obtain the nodal acceleration of the solid \mathbf{a}_S from the discretized form of Equation 2.
- 3) Velocities and momentum of the MPs are updated from nodal accelerations of each phase.
- 4) Nodal velocities are then calculated from nodal momentum and used to compute the strain rate at the MP location.
- 5) Liquid and soil constitutive laws give the increment of excess pore pressure and effective stress respectively.
- 6) Displacement and position of each MP is updated according to the velocity of the solid phase.

3 2-PHASE, DOUBLE-POINT FORMULATION

The 2-phase double-point formulation was initially presented by Bandara (2013) and Wieckowski (2013), and later extended by Abe et al. (2013) and Martinelli (2016). It assumes that the saturated porous media consist of a superposition of two independent continuum media, hence the solid skeleton and the liquid phase are represented separately by two sets of Lagrangian MPs: solid material points (SMPs) and liquid material points (LMPs). While SMPs moves attached to the solid skeleton, LMPs follow the liquid motion, both carrying properties of respective phases. As a result, the required number of MPs to discretize a saturated porous domain increases substantially (at least it doubles) compared to the single-point formulation.

An important advantage of this approach compared to the single-point formulation is that the mass of all MPs remains constant. Therefore, the conservation of both solid and liquid mass is fulfilled through the calculation.

Another important feature of the double-point formulation is that LMPs embodies either liquid within the pores or free liquid. According to this framework, Martinelli (2016) describes three possible domains:

- i) porous media in saturated conditions, when SMPs and LMPs share the same grid element,
- ii) porous media in dry conditions, when only SMPs are located in the grid element,
- iii) free liquid, when only LMPs are located in the grid element.

In any case, the dynamic behaviour of the continuum can be described with the solid and liquid dynamic momentum balances (Eq.6 and 7 respectively) which are solved at the nodes of the grid, being \mathbf{a}_S and \mathbf{a}_L the primary unknowns. Note that solid momentum balance is considered for convenience instead of momentum balance of the mixture. Solid and total mass balances (Eq.4 and 8 respectively) and constitutive relationships are posed at the corresponding MPs in order to update secondary variables.

$$n_S \rho_S \mathbf{a}_S = \nabla \cdot \bar{\boldsymbol{\sigma}}_S + \mathbf{f}^d + n_S \rho_S \mathbf{b} \quad (6)$$

$$n_L \rho_L \mathbf{a}_L = \nabla \cdot \bar{\boldsymbol{\sigma}}_L - \mathbf{f}^d + n_L \rho_L \mathbf{b} \quad (7)$$

$$\frac{D^L \varepsilon_{vol,L}}{Dt} = \frac{1}{n_L} [n_S \nabla \cdot \mathbf{v}_S + n_L \nabla \cdot \mathbf{v}_L + (\mathbf{v}_L - \mathbf{v}_S) \cdot \nabla n_L] \quad (8)$$

In the previous expressions, $\bar{\boldsymbol{\sigma}}_S = \boldsymbol{\sigma}' + n_S \boldsymbol{\sigma}_L$ and $\bar{\boldsymbol{\sigma}}_L = n_L \boldsymbol{\sigma}_L$ correspond to the partial stresses for solid and liquid phases respectively, $\boldsymbol{\sigma}'$ =effective stress tensor, and $\boldsymbol{\sigma}_L$ =stress tensor of the liquid phase (equivalent to pore pressure p in saturated porous media). $D^L(\cdot)/Dt$ denotes the material time derivative with respect to the liquid phase.

This formulation presents two additional differences compared to the single-phase approach. Both are related to the fact that the behaviour of the continuum described in the double-point framework can vary from dry porous media to pure fluid. This leads to extreme changes in flow regime and huge gradients of volumetric concentration ratios in transition zones.

The first one is that the drag force \mathbf{f}^d is generalized and Equation 5 is extended in order to account for laminar and steady flow in high velocity regime (Forchheimer, 1901), leading to Equation 9 where β is the non-Darcy flow coefficient (Ergun, 1952) and can be computed with Equation 10

$$\mathbf{f}^d = \frac{n_L^2 \mu_L}{\kappa_L} (\mathbf{v}_L - \mathbf{v}_S) + \beta n_L^3 \rho_L |\mathbf{v}_L - \mathbf{v}_S| (\mathbf{v}_L - \mathbf{v}_S) + \boldsymbol{\sigma}_L \cdot \nabla n_L \quad (9)$$

$$\beta = B / \sqrt{\kappa_L A n_L^3} \quad (10)$$

Moreover, the intrinsic permeability κ_L is computed and updated as a function of the effective porosity n_L with the Kozeny-Carman formula (Bear, 1972):

$$\kappa_L = \frac{D^2}{A} n_L^3 / (1 - n_L)^2 \quad (11)$$

The second difference recalls in the liquid mass balance (Eq.8). Now, all convective terms are accounted including the spatial variations of liquid volumetric concentration ratio ($(\mathbf{v}_L - \mathbf{v}_S) \cdot \nabla n_L$), hence liquid fluxes due to changes in porosity are accounted. Liquid is also considered weakly compressible.

This formulation can distinguish between mixtures characterized by low and high porosities (see Figure 2). Figure 2a shows a low-porosity mixture, where the grains of the solid skeleton are in contact and the behaviour can be described by constitutive models developed for granular materials (solid-like response). Conversely, as shown in Figure 2b, in a high-porosity mixture the grains are not in contact and float together with the liquid phase. In this case, the effective stresses are equal to zero and the response of the mixture is described by the Navier-Stokes equation (liquid-like response).

In the current formulation, the two aforementioned states are distinguished through the maximum porosity n_{max} of the SMP, which is the maximum value of the porosity for a given soil in its loosest state. During the fluidization process, when the mixture porosity is lower than the maximum porosity ($n_L = 1 - n_S < n_{max}$), the decrease in the mean effective stress results in increase in the porosity. When the contact forces between the grains vanish, the mean effective stress becomes nil. However, the fluidization occurs only if the grains are significantly separated, so that the porosity of the SMP is larger than n_{max} . In the reverse process, i.e. the sedimentation of a fluidized mixture, the porosity decreases due to the fact that the solid grains get closer to each other. However, the effective stresses recur only if the porosity is smaller than n_{max} , i.e. the grains are close enough to be in contact.

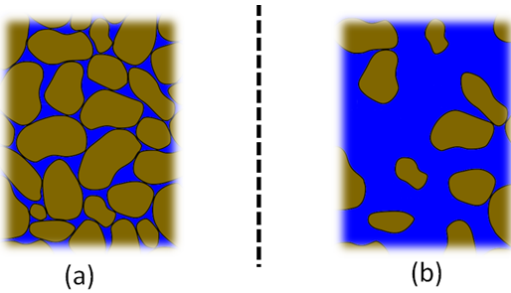


Figure 2 Solid-liquid mixture with (a) low porosity (solid-like response) and (b) high porosity (liquid-like response).

Equation 7 is used to describe the behavior of water in the soil-water mixture. In case of liquid-like response, the deviatoric part of the stress tensor of the liquid is computed using the liquid strain rate tensor and a viscosity which takes into account the solid concentration ratio of the mixture. In case of solid-like behavior the deviatoric stress tensor is set to zero.

In this formulation, all LMPs belonging to the liquid free surface are detected and the liquid stress is set to zero to these material points.

The MPM solution scheme for each time step can be summarized as follow:

- 1) Nodal acceleration of the liquid \mathbf{a}_L is calculated by solving the discretized form of Equation 7.
- 2) Nodal acceleration of the solid \mathbf{a}_S is calculated by solving the discretized form of Equation 6.
- 3) Velocities and momentum of the MPs are updated from nodal accelerations of each phase.
- 4) Nodal velocities are then calculated from nodal momentum and used to compute the strain rate at the MP location.
- 5) Liquid and soil constitutive laws give the increment of liquid stress and effective stress respectively in LMP and SMP.
- 6) All LMPs that belong to the liquid free surface are detected.
- 7) Displacement and position of each MP is updated according to the corresponding velocity field.

The double-point formulation has been used to simulate the submerged column collapse (Martinelli and Rohe, 2015), the fluidization of a vertical column test (Bolognini et al., 2017), the interaction between water jet and soil bed (Liang et al. 2017), the simulation of the crater development around a damaged pipeline (Martinelli et al. 2017a), and a dike failure (Martinelli et al., 2017b). Other applications are also presented in Martinelli (2016).

4 EXAMPLES

Two numerical examples are presented in this section. The first one is a 1D consolidation problem, and the aim of it is to validate both theories with an analytical solution. The second example considers the collapse of a saturated sand column and shows the importance of considering the mobility of the two phases separately and the spatial and temporal variation of the volumetric concentration ratios n_L and n_S .

4.1 1D consolidation

The two 2-phase formulations are validated by means of the problem of one dimensional consolidation for which an analytical solution by Terzaghi exists for the case of small deformations. In this case, the assumptions of laminar liquid flow through the pores, constant volumetric concentration and permeability are well satisfied.

A 1m-column of saturated weightless, linear-elastic material is considered (Tab. 1). The column is discretised with 40 rows of 6 tetrahedral elements. Standard oedometric boundary conditions are applied, the base of the column is impermeable and the top is permeable. Each element contains 4 MPs (single-point formulation) or 4 LMPs and 4 SMPs (double-point formulation). Note that the number of MPs required to discretize the problem doubles in the double-point analysis.

A total load of 10 kPa is applied at the top of the column. The initial pore pressure is $p_0 = 10$ kPa and the initial effective stress is 0. Subsequently, the water is allowed to drain out of the top surface. Gradually, the load redistributes from the pore pressure to the soil skeleton.

This example considers a seepage problem in a homogeneous media at small deformations, thus the intrinsic permeability is assumed constant throughout the simulation and the second term of Equation 9 can be neglected.

Figure 3 shows the change of normalized pore pressure over the normalized height of the column with time for selected MPs. The dimensionless time factor T is defined as:

$$T = \frac{c_v t}{h^2} \quad (12)$$

with c_v = consolidation coefficient, h = height of the column.

The results of both formulations are in excellent agreement with the analytical solution, thus validating the implementation.

In this example the single-point and the double-point formulation give the same results, i.e. they are both well applicable when the fluid flow is laminar and the spatial variability of the porosity is negligible, which is the case of many seepage problems in engineering.

Table 1 Material parameters

Parameter		Value
Initial porosity [-]	n_L	0.4
Grain density [kg/m ³]	ρ_S	2650
Liquid density [kg/m ³]	ρ_L	1000
Intrinsic permeability [m ²]	κ_L	1.0214e-10
Dynamic viscosity [kPa s]	μ_L	1.002e-6
Young modulus [kPa]	E	10000
Poisson ratio [-]	ν	0.2
Fluid bulk modulus [kPa]	K_L	21500
Consolidation coefficient [m ² /s]	c_v	1.1

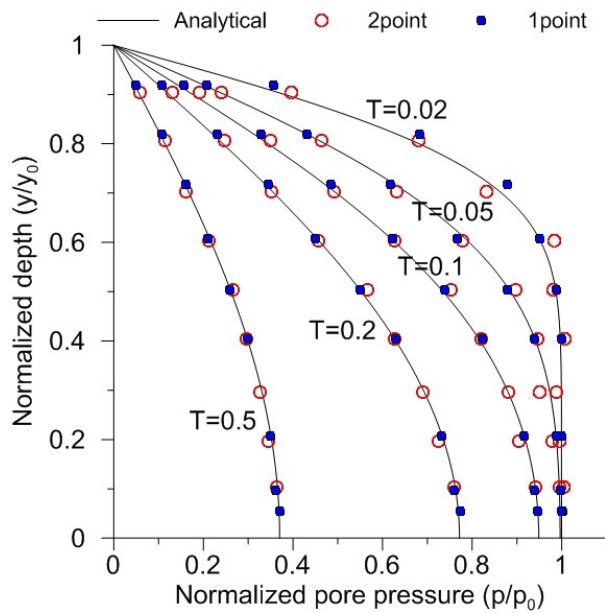


Figure 3 Results of 1D consolidation problem

4.2 Column collapse

In this section, we consider the collapse of a column of saturated soil in air. This problem is well suited to highlight the differences between the two approaches considered in this study.

The geometry is shown in Figure 4, a 1m-wide 2m-high column, subjected to gravity is allowed to collapse on a flat surface. All the boundaries of the model are impermeable. The bottom boundary is fully fixed, while roller boundary conditions are applied at the remaining surfaces. The width of the model perpendicular

to the xy-plane of Figure 4 is 0.2m and it is discretized with only one row of elements to simulate quasi-2D conditions with a full 3D code.

A standard linear elastic perfectly plastic constitutive model with a Mohr-Coulomb failure criterion is used for the solid skeleton and a standard Newtonian compressible constitutive model is used for water. The material parameters are listed in Table 2. Initial effective stresses are generated via K_0 procedure and the pressure distribution is assumed hydrostatic.

In both formulations, tensile stress is not allowed in the liquid by setting a cavitation threshold to 0kPa, this prevents numerical problems with traction stresses in the double-point formulation which will be further investigated in the future.

Figure 5 shows the results obtained with the single-point formulation. The motion is driven by gravity: a shear surface develops and part of the soil accelerates flowing on the flat surface; kinetic energy is dissipated by friction inside the soil mass and at the base and by the drag force. Finally, the material decelerates and stops.

With the single-point formulation the MPs carry the information of both solid and liquid, thus the material is assumed to be fully saturated throughout the computation. In contrast, the double-point formulation allows large relative movements between SMPs and LMPs and thus the separations between the phases (Fig. 6).

During the column collapse using the double-point approach, SMPs move ahead with respect to LMPs developing a granular front and a small layer of dry material can be recognized at the surface (Fig. 6). This phenomenon is often recognized in debris flow (Gray et al. 2009, Johnson et al. 2012, Pudasaini 2012). Recently, it has been shown that the formation of a fluid front, i.e. the liquid moves ahead of the solid, or a granular front depends on the shear rate of the moving mass, the characteristics of the grain assembly (e.g. particle concentration) and the viscosity of the fluid (Leonardi et al. 2015).

In the implemented double-point formulation, the effect of partial saturation, e.g. suction, in the behaviour of elements filled only with solid MPs is not considered, thus the soil is assumed to be dry.

Figure 7 shows the liquid volumetric concentration ratio (n_L) at different time instants. It is null in the dry part of the soil; moreover, it should be noted that it varies significantly in space and time (Fig. 7). For this reason, the term ∇n_L should not be neglected in the governing equation of motion (Eq. 8).

During column collapse, the solid concentration decreases along the superficial and front part of the moving mass, because solid grains tend to separate. When they are no longer in contact between each other the effective stresses nullify and the soil is in a liquefied state. The transition between the solid and the liquefied state is controlled by a maximum porosity of $n_{max} = 0.5$. Figure 8 shows with blue dots the

solid MP which are in a liquefied state, i.e. for which the effective stress is null.

Comparing Figures 5 and 6 it can be noted that the simulations with the single-point formulation predicts longer runout of the soil mass. This is probably due to the underestimation of the drag force (Eq. 5) because the assumption of the validity of Darcy's law is not satisfied in this case.

The definition of the drag force is a key issue in this type of problems. Figure 9 compares the results obtained considering a material with a reference solid particle diameter $d=7\text{mm}$ and using a drag force computed as follows:

- Neglecting the quadratic term in Equation 9, i.e. the second addend, and assuming $\kappa_L=\text{constant}$ (Fig. 9a)
- Neglecting the quadratic term in Equation 9, and updating the intrinsic permeability using Equation 11 (Fig. 9b);
- Considering the full form of Equation 9, and updating the intrinsic permeability using Equation 11 (Fig. 9c).

It can be seen that the movement of the liquid phase differs significantly in the considered cases.

Table 2 Material parameters (** applicable only for the single-point formulation, *applicable only for the double-point formulation)

Parameter		Value
Initial porosity [-]	n_L	0.4
Grain density [kg/m^3]	ρ_S	2650
Liquid density [kg/m^3]	ρ_L	1000
Intrinsic permeability [m^2]	κ_L	$1.021\text{e-}10^{**}$
Dynamic viscosity [kPa s]	μ_L	$1.002\text{e-}6$
Young modulus [kPa]	E	10000
Poisson ratio [-]	ν	0.2
Fluid bulk modulus [kPa]	K_L	21500
K_θ coefficient [-]	K_θ	0.5
Ref. grain size diameter [mm]	d	2^*
Ergun parameter	A	150^*
Ergun parameter	B	1.75^*
Maximum porosity	n_{max}	0.5^*

5 DISCUSSION AND CONCLUSIONS

This paper presents and compares two recently proposed approaches to simulate multiphase problems with MPM, i.e. 2-phase single-point formulation and 2-phase double-point formulation.

2-phase granular-fluid mixture flows are characterized primarily by the relative motion and interaction between the solid and fluid phases. Drag is one of the very basic and important mechanisms of two-phase flow as it incorporates coupling between the phases. The drag force used in the applied double-point formulation considers the gradient of the volumetric phase concentration, a linear (laminar-type, at low velocity) and quadratic (nonlinear-type, at high velocity) contribution. In contrast, the drag force used in the single-point formulation assumes the validity of the Darcy law, thus it is only valid when the fluid motion inside the pores is laminar.

The single-point and the double-point formulations are equivalent and both are well applicable to seepage problems when the fluid velocity is low and the spatial variability of solid concentration is negligible. However, because the number of MPs required to discretize the saturated media is much larger in the double-point formulation, the single-point formulation can be slightly more efficient.

In contrast, the use of double-point formulation is necessary when flow velocity and variability of concentrations are relevant. Moreover, interaction between porous media and free liquid can be captured. This is an important feature in many problems such as the study of debris flow propagation, dike stability, erosion and scouring and other coastal applications.

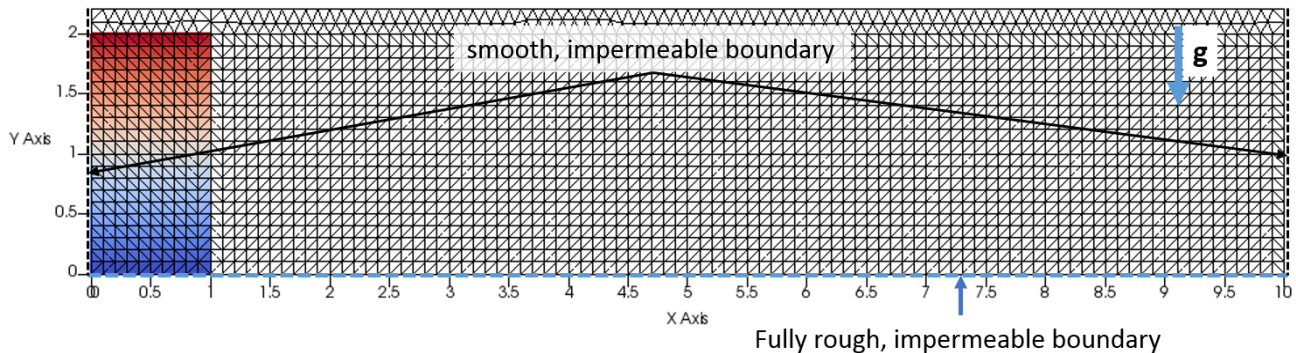


Figure 4 Geometry and discretization of the column collapse problem.

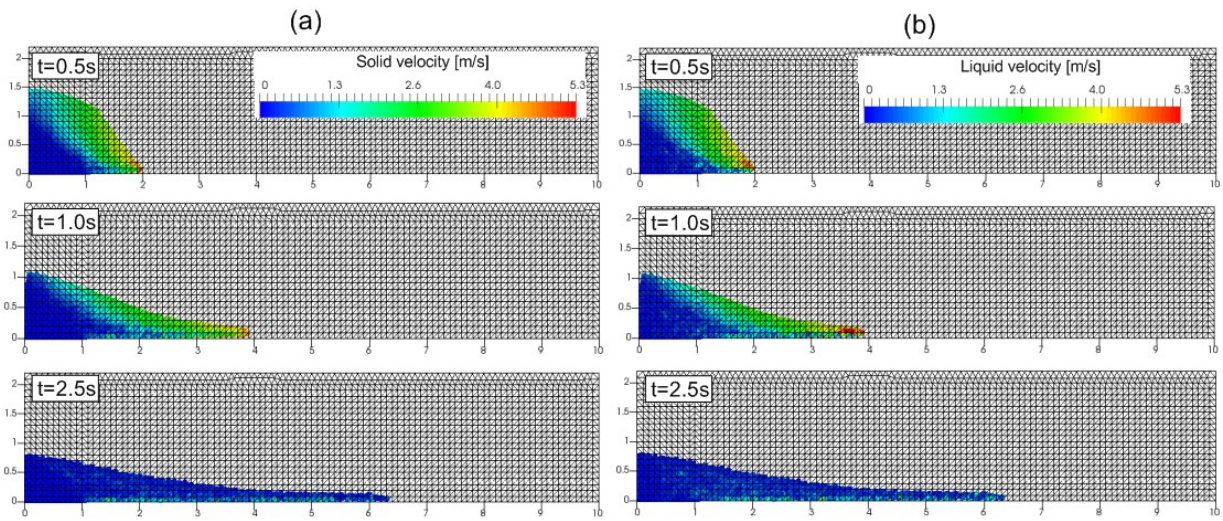


Figure 5 2-phase single-point formulation. (a) solid velocity, (b) liquid velocity.

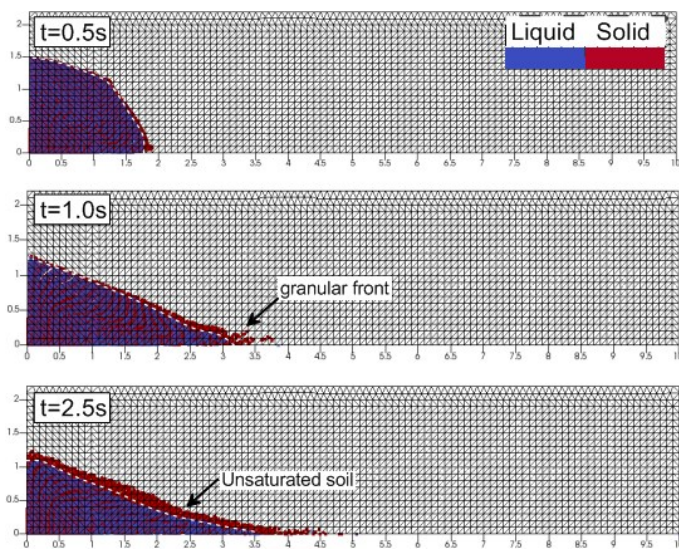


Figure 6 SMP and LMP with the double-point formulation

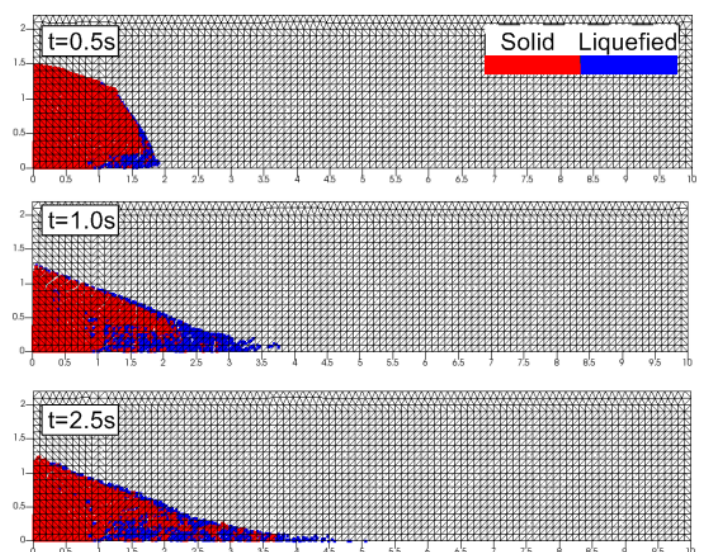


Figure 8 Phase status of SMP during column collapse.

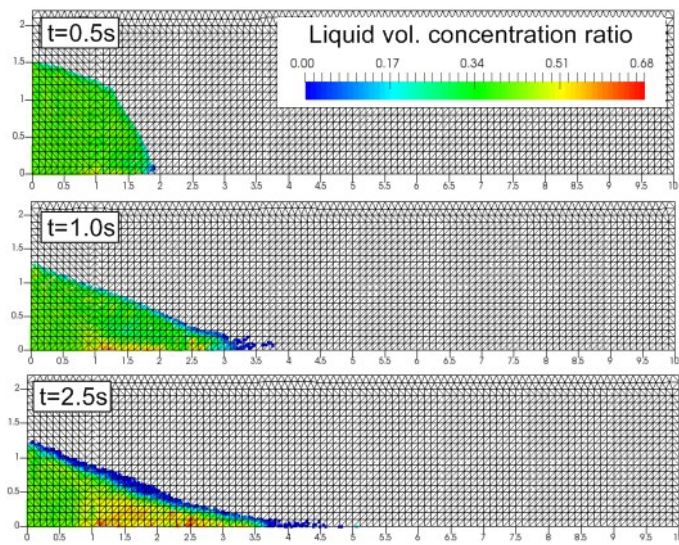


Figure 7 Liquid volumetric concentration ratio at the LMP.

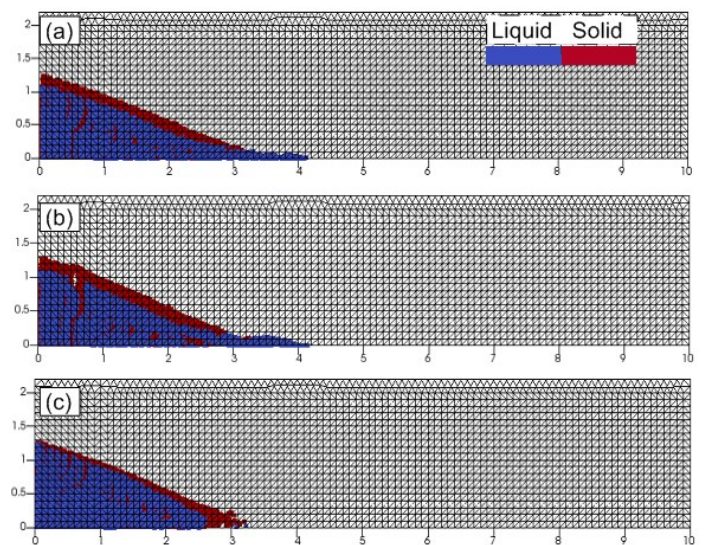


Figure 9 Effect of drag force equation on the SMP and LMP position at $t=0.85s$: (a) linear term only, $\kappa_L = \text{const.}$; (b) linear term only, $\kappa_L \neq \text{const.}$; (c) linear and quadratic term, $\kappa_L \neq \text{const.}$

6 REFERENCES

- Abe, K., Soga, K., Bandara, S. 2014. Material point method for coupled hydromechanical problems. *Journal of Geotechnical and Geoenvironmental Engineering* 140 (3): 1–16.
- Alonso, E. E., Pinyol, N. M. & Yerro A. 2014. Mathematical Modelling of Slopes. *Procedia Earth and Planetary Science* 9: 64–73.
- Bandara, S. 2013. Material point method to simulate large deformation problems in fluid-saturated granular medium. *PhD thesis, University of Cambridge, Cambridge, UK.*
- Bandara, S. & Soga, K. 2015. Coupling of soil deformation and pore fluid flow using material point method. *Computers and Geotechnics* 63(1): 199–214.
- Bear, J. 1972. Dynamics of fluids in porous media. Elsevier.
- Bolognini, M., Martinelli, M., Bakker, K.J., Jonkman, S.N. 2017. Validation of material point method for soil fluidisation analysis. *Journal of Hydrodynamics* 29(3): 431–437.
- Ceccato, F., Beuth, L., Simonini, P. 2016a. Analysis of piezocone penetration under different drainage conditions with the two-phase material point method. *Journal of Geotechnical and Geoenvironmental Engineering* 142(12).
- Ceccato, F. & Simonini, P. 2016b. Numerical study of partially drained penetration and pore pressure dissipation in piezocone test. *Acta Geotechnica* (published online).
- Ergun, S. 1952. Fluid flow through packed column. *In Chemical Engineering Progress.*
- Forchheimer, P. 1901. Wasserbewegung durch Boden. *Z Ver Deutsch Ing* 45: 1782–1788.
- Galavi, V., Beuth, L., Coelho, B.Z., Tehrani, F.S., Hölscher P. & Van Tol, F. 2017. Numerical Simulation of Pile Installation in Saturated Sand Using Material Point Method. *Procedia Engineering* 175: 72–79.
- Gray, J. & Ancey, C. 2009 Segregation, recirculation and deposition of coarse particles near two-dimensional avalanche fronts. *Journal of Fluid Mechanics* 629: 387–423.
- Jassim, I., Stolle, D., Vermeer, P.A. 2013. Two-phase dynamic analysis by material point method. *International Journal for Numerical and Analytical Methods in Geomechanics* 37(15): 2502–2522.
- Johnson, C.G, Kokelaar, B.P, Iverson, R.M., Logan, M., Lahusen, R.G. Gray, J.M.N.T. 2012. Grain-size segregation and levee formation in geophysical mass flows, *Journal of Geophysical Research* 117, F01032.
- Leonardi, A., Cabrera, M., Wittel, F.K., Kaitna, R., Mendoza, M., Wu, W., Herrmann, H. J. 2015. Granular-front formation in free-surface flow of concentrated suspensions. *Physical Review E* 92(5), 052204.
- Liang, D., Zhao, W., Martinelli, M. 2017. MPM simulations of the interaction between water jet and soil bed. *Procedia Engineering* 175: 242–249.
- Martinelli, M. & Rohe, A. 2015. Modelling fluidisation and sedimentation using material point method. *1st Pan-American Congress on Computational Mechanics.*
- Martinelli, M. 2016. Soil-water interaction with Material Point Method. Double-Point Formulation. *Report on EU-FP7 research project MPM-Dredge PIAP-GA-2012-324522.*
- Martinelli, M., Tehrani, F.S., Galavi, V. 2017a. Analysis of crater development around damaged pipelines using the material point method, *Procedia Engineering* 175: 204–211.
- Martinelli, M., Rohe, A., Soga, K. 2017b. Modeling dike failure using the material point method. *Procedia Engineering* 175: 341–348.
- Pudasaini, S.P. 2012. A general two-phase debris flow model, *Journal of Geophysical Research* 117, F03010.
- Soga, K., Alonso, E., Yerro, A., Kumar, K., Bandara, S. 2016. Trends in large-deformation analysis of landslide mass movements with particular emphasis on the material point method. *Géotechnique* 66 (3): 248–273.
- Sulsky, D., Chen, Z., Schreyer, H.L. 1994. A particle method for history-dependent materials. *Computer Methods in Applied Mechanics and Engineering* 118(1–2): 179–196.
- Wieckowski, Z. 2013. Two-phase numerical model for soil-fluid interaction problems. *In Proceedings of ComGeoIII* pp.410–41.
- Yerro, A., Alonso, E., Pinyol, N. 2015. The material point method for unsaturated soils. *Géotechnique* 65(3), 201–217.
- Yerro, A., Alonso, E. E., Pinyol, N.M. 2016. Run-out of landslides in brittle soils. *Computers and Geotechnics* 80: 427–439.
- Zabala, F. & Alonso, E.E. 2011. Progressive failure of Aznalcólar dam using the material point method. *Géotechnique* 61(9): 795–808.